Spatiotemporal heterogeneity of larch budmoth outbreaks in the French Alps over the last 500 years

Mélanie Saulnier, Alain Roques, Frédéric Guibal, Philippe Rozenberg, Ginette Saracco, Christophe Corona, Jean-Louis Édouard

Spatiotemporal heterogeneity of larch budmoth outbreaks in the French Alps over the last 500 years

M. Saulnier, A. Roques, F. Guibal, P. Rozenberg, G. Saracco, C. Corona, and J.-L. Edouard

Abstract: In the subalpine forest ecosystems of the French Alps, European larch trees (*Larix decidua* Mill.) are periodically affected by outbreaks of a defoliating insect, the larch budmoth (*Zeiraphera griseana* (Hübner, 1799); LBM). To assess the long-term dynamics of LBM populations, we propose a spatiotemporal analysis of a long outbreak chronology reconstruction for the entire French Alps covering the period 1414–2009. This chronology was obtained by analyzing tree ring width (TRW) chronologies collected from 44 larch populations. The evidence of a latitudinal gradient in LBM is an original result that we have related to the "travelling waves" and "epicenter" theory. Wavelet analyses revealed a strong explicit continuous signal for periodicities of 4, 8, and 16 years throughout the entire 1500–2003 time series, except for a loss of power from 1690 to 1790 and since the early 1980s. We hypothesize that these abrupt changes could reflect a physiological response of LBM to past climatic variations. The spatial and temporal variability of LBM outbreaks and the propagation phenomenon in the French Alps highlighted by this study raises questions regarding its future dynamics in response to the expected climate change.

Key words: larch budmoth, insect outbreak, French Alps, spatiotemporal heterogeneity, climate change impact.

Résumé : Dans les écosystèmes forestiers subalpins des Alpes françaises, le mélèze (*Larix decidua* Mill.) subit périodiquement les épidémies d'un insecte défoliateur, la tordeuse du mélèze (*Zeiraphera griseana* (Hübner, 1799); LBM). Afin de mieux comprendre les dynamiques à long terme des populations de tordeuse, nous proposons dans cet article une analyse spatio-temporelle d'une très longue reconstruction des épidémies pour la période 1414–2009 sur l'ensemble des Alpes françaises. Cette chronologie a pu être reconstruite à partir des cernes de croissance de 44 populations de mélèze. Les résultats ont permis de mettre en évidence le rôle d'un gradient latitudinal que nous avons attribué au phénomène théorique des « épicentres » et « vagues de dissémination ». D'autre part, les analyses temporelles, réalisées à l'aide de la méthode des ondelettes, ont révélé l'existence d'un fort signal continu pour des fréquences périodiques de 4, 8 et 16 ans sur l'ensemble de la chronologie à l'exception d'une perte d'énergie entre 1690 et 1790 et depuis le début des années 1980. Ces changements pourraient refléter une réponse physiologique de la tordeuse à des variations climatiques passées. La variabilité temporelle et spatiale des épidémies de tordeuse ainsi que le mode de propagation à travers les Alpes françaises nous ont conduits à nous interroger sur les dynamiques futures de l'insecte et de son hôte en réponse au réchauffement climatique rapide dans les écosystèmes de haute élévation.

Mots-clés : tordeuse des bourgeons du mélèze, épidémies d'insecte, Alpes françaises, hétérogénéité spatio-temporelle, impact du changement climatique.

Introduction

Outbreaks of defoliator insects are major disturbance events in forests around the world, especially in high-latitude and high-elevation ecosystems. Depending on their intensity, such outbreaks may lead to complete tree defoliation and, sometimes, tree mortality. Although insect damage has been considered as less prevalent in forests of Eurasia compared with those of North America (Kneeshaw et al. 2015), outbreaks of European insect species that exhibit eruptive population dynamics may result in highly significant ecological and economic consequences (Jepsen et al. 2008; Lindner et al. 2010). Currently, a large number of forest defoliators, especially moths and sawflies, exhibit population cycles, with outbreaks occurring at more or less regular intervals (Berryman 1988). The analysis of the dynamics of these outbreaks had long been limited to the description of the population demographic trends (Berryman 1988). With the development of new technologies and analytical methods, several studies have focused on the complex mechanisms that might explain outbreak parameters such as occurrence and recurrence and their spatiotemporal dynamics (Bjørnstad et al. 2002; Ranta et al. 2002; Esper et al. 2007; Delamaire 2009). The recent elevational range shift mediated by climate change reported in plants (Sturm et al. 2001; Cleland et al. 2007; Lenoir et al. 2008; Engler et al. 2011; Dullinger et al. 2012),

tree lines (Saulnier 2012), and insects (Parmesan 1996, 2006; Battisti et al. 2005, 2006; Robinet and Roques 2010; Battisti and Larsson 2015) is also of growing concern because it could affect plant–insect relationships. Climate change has been claimed to be responsible for the range expansion northwards and upwards of several species of insect defoliators in temperate and boreal forests in Europe (Battisti et al. 2005; Jepsen et al. 2008; Roques 2015). However, the effects on population dynamics do not seem to be so unilateral; some insects respond by increasing the level of leaf consumption and consequently the defoliation, whereas others show higher mortality and lower performance (Battisti 2008). Thus, in some defoliators, climate change may be expected to result in increased spatial expansion and more severe outbreaks (Fleming and Candau 1998; Logan et al. 2007; Volney and Fleming 2000; Williams and Liebhold 1995). It is hypothesized that the regions that represent the northern or upper limits of occurrence of such defoliator species such as the Alps or the boreal zone may face an increase in population density of these insects (Lindner et al. 2010; Netherer and Schopf 2010).

In contrast, it is hypothesized that warming may alter and even lead to a collapse of the population cycles in certain other species such as the larch budmoth (*Zeiraphera griseana* (Hübner, 1799); =*Z. diniana* Guenée 1845, according to Fauna Europaea (http://www.fauna-eu.org), hereafter abbreviated as LBM) (Esper et al. 2007; Johnson et al. 2010; Ims et al. 2008; Allstadt et al. 2013). Understanding the mechanisms of cycle collapse has proven to be challenging because of limited long-term data on the populations of such cyclical species. With some exceptions (Büntgen et al. 2009; Johnson et al. 2010), the scarce long-term records are in fact insufficient to (*i*) confirm robustly the changes in the patterns of the population dynamics and (*ii*) detect causal factors with certainty.

Therefore, an attempt to elucidate the response to climate change of LBM, one of the most well-known cyclical forest insects, is of general interest. Currently, LBM presents periodic larval outbreaks, which result in widespread reddening of the subalpine forests of European larch (*Larix decidua* Mill.) in the Alps. The annual variations in LBM population density have been thoroughly surveyed since the late 1950s throughout the Alps, from the southern French Alps to Switzerland and Austria (Auer 1977; Baltensweiler et al. 1977; Roques and Goussard 1982; Baltensweiler and Fischlin 1988; Dormont et al. 2006). These studies tended to evidence the occurrence of 8- to 10-year cycles of LBM outbreaks. However, this outbreak periodicity was only observed at an elevation of 1800–2000 m above sea level (a.s.l.), considered as optimal for the synchronization of LBM egg hatching with the appearance of larch needles (Baltensweiler et al. 1977).

LBM defoliation sharply reduces the width of tree rings in larch host trees during the outbreak period (Esper et al. 2007). Thus, dendrochronological studies focused on LBM impact on larch tree rings at different spatial scales confirmed the 8- to 10-year periodicity for the Alpine region (Büntgen et al. 2009) and at the regional level in the Swiss Alps (Esper et al. 2007; Baltensweiler et al. 2008), the French Alps (Rolland et al. 2001; Delamaire 2009), and the Italian Alps (Motta 2004; Nola et al. 2006). The longest available dendrochronological reconstruction of outbreaks showed fluctuations persisting over the past 1173 years in the Swiss Alps, with population peaks occurring every 9.3 years on average (Esper et al. 2007) and with only a few apparent gaps. Furthermore, many studies have looked at the spatial dynamics of the outbreaks (Ranta et al. 2002; Rolland et al. 2001; Baltensweiler and Rubli 1999) and described a pattern based on the travelling waves and epicenter theory (Bjørnstad et al. 2002; Johnson et al. 2004).

However, since the 1980s, several authors have reported rapid changes in LBM population cycles, which may have major consequences for both the regularity and range of the oscillations (Esper et al. 2007; Johnson et al. 2010). The 1800–2000 m a.s.l. optimum zone of regular outbreak occurrence was thus suspected to have shifted towards higher elevations since the 1990s. A similarly rapid change in elevational distribution has been observed in other insects such as the pine processionary moth (*Thaumetopoea pityocampa* (Denis & Schiffermüller, 1775)) in response to climate warming (Battisti et al. 2006; Roques 2015).

The aim of this paper is to propose a long-term reconstruction of LBM outbreak events over the whole of the French Alps and to test their spatiotemporal regularity during the last 500 years. We hypothesize that such an approach offers a better basis for understanding the dynamics of disturbances and host–insect interactions by addressing the following questions. (*i*) Is it possible to localize the epicenter of the outbreak events? (*ii*) Is the periodicity of the LBM outbreaks constant? (*iii*) Do the changes in LBM outbreaks in response to global change occur at the scale of the whole of the French Alps?

Materials and methods

Study area

The sampling network consisted of 620 individual tree ring width (TRW) series from 44 populations (Fig. 1) spanning the period from 933 to 2009. This large dataset results from successive studies conducted in the French Alps since 1974 (Serre 1978; Tessier 1986; F. Guibal, unpublished; Edouard et al. 2002, 2009, 2010; Corona et al. 2011; Saulnier 2012). The sites were selected to cover the north–south and west–east climatic gradients (44°06′N to 45°53′N, 6°40′E to 7°45′E; Fig. 1) in the French Alps. The sampled sites extended from low to high elevations (1050–2300 m a.s.l.), consisting of open forest stands with various slope exposures. Although human activities largely molded the French Alps, they occurred in a disjointed and asynchronous way. We therefore assumed that the use of this extensive network would enable us to minimize the effects of human disturbances.

Tree ring data and dendrochronological analysis

At each site, 5–37 undamaged dominant or co-dominant living trees were selected. From each tree, at least two cores were sampled in opposite directions parallel to contour lines, approximately 1.30 m above ground level, using a Swedish increment borer. In the laboratory, cores were mounted on wooden supports so that the cross-sectional view was facing up. Samples were then sanded using increasingly finer grade sandpaper and smoothed with a razor blade or by sanding with progressively finer grade sandpaper to optimal surface resolution, allowing annual rings to be recognized easily under magnification (Fig. 2). They were then processed using standard procedures for tree ring analysis (Stokes and Smiley 1968; Fritts 1976; Cook et al. 1990; Speer 2010). Missing and wedging rings are common features of larch secondary growth. Cores were cross-dated under a binocular microscope by identifying marker years and specific ring-width patterns. Narrow rings provided the primary visual markers; rings with thin or light latewood were also used. Marker years and specific patterns were recorded using the skeleton plot technique (Stokes and Smiley 1968). Once cross-dated, ring-width series were measured to the nearest 0.01 mm. To remove age-associated trends and minimize the influence of nonclimatic variations, the TRW series from the individual trees were standardized (Fritts 1976) using ARSTAN software (Cook and Holmes 1984). A double-detrending process was applied, based on an initial negative exponential or linear regression, followed by a fitting of a 25-year cubic smoothing spline with a 50% frequency cutoff. Dimensionless indices were obtained by dividing the observed ring width value by the predicted one. This process — well-suited to the conservation of high-frequency signals, i.e., abrupt growth decrease expected to occur in response to disturbance such as defoliation by LBM (Saulnier 2012) — creates stationary time series for each tree with a mean of 1 and homogeneous variance (Cook and Peters 1981; Cook et al. 1990).

Fig. 1. Spatial distribution of the 44 populations. [Colour online.]

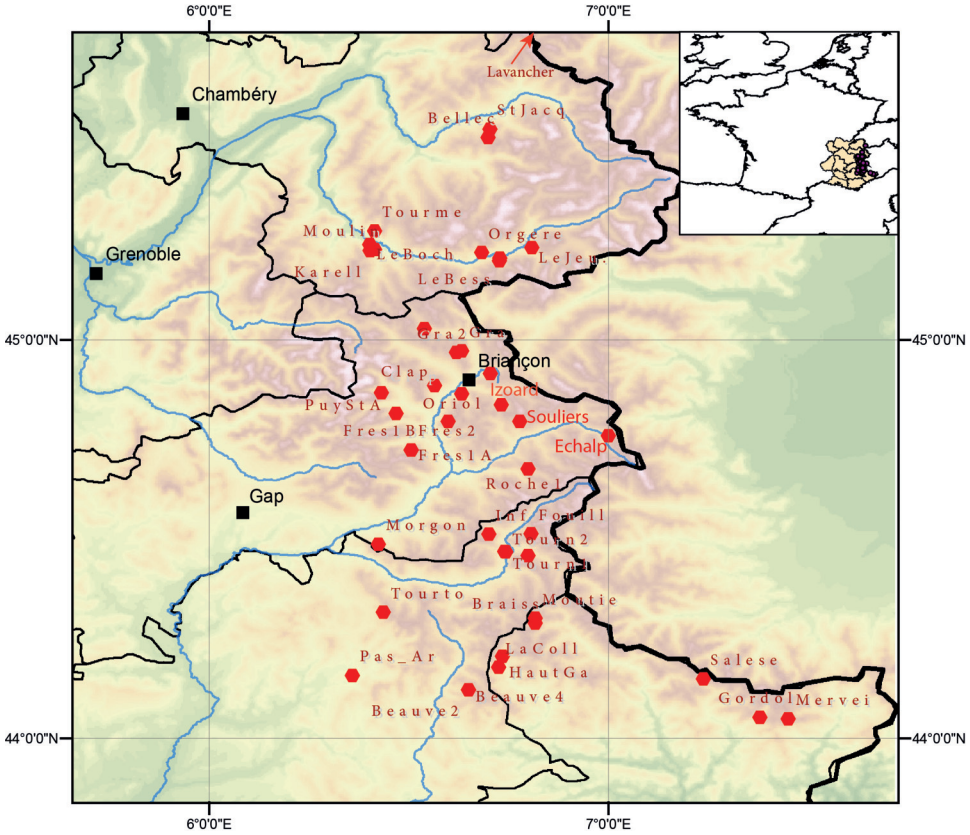

Fig. 2. This photograph illustrates the impact of the 1856 outbreak on a tree ring series from a dominant larch located in Puy-Saint-Vincent stand, Hautes-Alpes, France. The ring with double dots (far right) is year 1850; the ring of year 1860 has a single dot (left); the ring of year 1856 is a very narrow light ring with a very thin latewood following a wide ring (1855); and the ring of year 1857 is slightly thinner than the ring of year 1856. [Colour online.]

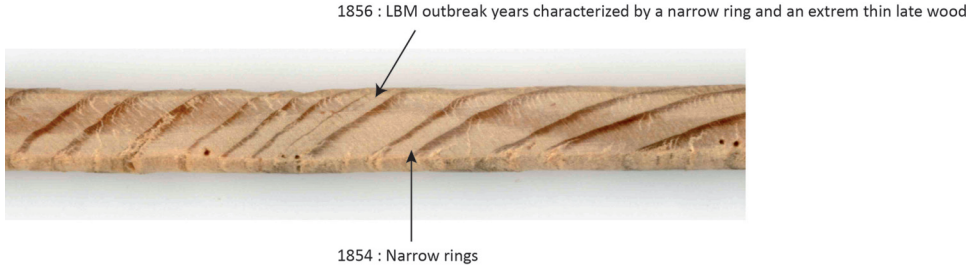

Several descriptive statistics commonly used in dendrochronology were computed to check the common signal recorded by the chronologies and are summarized in Table 1. These include standard deviation (SD), which estimates the variability of measurements for the whole series, and mean sensitivity (MS), which represents the mean of the relative deviations between consecutive rings for a given chronology. Both SD and MS allowed assessment of high-frequency variations in the chronologies (Fritts 1976). The first-order serial autocorrelation was computed to detect the persistence retained before and after the detrending. The mean correlation between trees (r_{bt}) was used as a measure of the strength of the common signal (Wigley et al. 1984) in each population. The r_{bt} was calculated as a mean correlation between all overlapping pairs of indexed tree series.

LBM outbreak reconstructions

Identification of LBM outbreaks was based on a comparison of larch chronologies with those of sympatric tree species used as references. The choice of the reference species is a crucial step in the analysis. Certain requirements must be met for the non-host species to be suitable (Swetnam et al. 1985): (*i*) have a climate response similar to that of the host species (Nola et al. 2006), (*ii*) not benefit in some manner from defoliation of the host tree, and (*iii*) not have been affected by other pests or other nonclimatic factors. In fact, the responses of the other alpine conifers to climate could be quite different from those of larch, even when they grow in the same forest (Weber 1997; Petitcolas and Rolland 1998; Rolland et al. 2001; Carrer and Urbinati 2004). Nevertheless, Saulnier (2012) showed that larch and stone pine (*Pinus cembra* L.) presented a similar response to mean temperature during the growth season. In the Alps, stone pine can also be infested by LBM, but the larvae develop on shoots, instead of needles as in larch (Baltensweiler et al. 1977). Belonging to a specific host-race, LBM pine populations also present a cyclical dynamic, peaking the same year or one year after the LBM larch populations (Dormont

Table 1. Site location and descriptive statistics of the stone pine tree ring chronologies.

Population	Label	Latitude, °N	Longitude, °E	Elevation, m a.s.l.	MRW, mm	SD	AC	*n*	Time period	Mean tree age, years	AC b.s	MS	r_{bt}
Beauvezer_2*****	1	44.12	6.65	1950	0.684	0.325	0.756	8	1421–1993	355	0.211	0.2	0.4
Beauvezer_4*****	2	44.12	6.65	1950	0.497	0.182	0.655	22	1160–1994	292	0.143	0.2	0.4
Bellecote***	3	45.51	6.70	2030	1.607	0.635	0.634	12	1812–1993	95	0.186	0.3	0.6
Braisse*	4	44.29	6.82	2150	0.801	0.360	0.720	16	1417–1995	391	0.238	0.2	0.7
Chardonnet*	5	45.03	6.54	2180	0.679	0.363	0.715	18	1492–1989	373	0.234	0.3	0.6
Clapouse**	6	44.87	6.43	2150	0.774	0.358	0.705	16	1557–1995	290	0.271	0.3	0.6
Echalp*	7	44.76	7.00	1930	0.803	0.445	0.730	32	1338–1995	342	0.393	0.3	0.7
Fouillouse**	8	44.51	6.81	2300	0.992	0.411	0.692	13	1669–1981	189	0.242	0.3	0.5
Fres1A*	9	44.73	6.51	1930	0.712	0.350	0.706	11	1632–1990	267	0.358	0.3	0.6
Fres1B*	10	44.73	6.51	1930	0.801	0.526	0.816	10	1542–1961	374	0.439	0.3	0.7
Fres2*	11	44.73	6.51	2100	0.916	0.460	0.733	18	1474–1992	357	0.311	0.3	0.6
Gordolasque**	12	44.06	7.38	1750	1.440	0.715	0.717	10	1830–1983	113	0.391	0.3	0.7
Granon1***	13	44.97	6.63	2230	0.877	0.429	0.718	12	1710–1993	229	0.388	0.3	0.7
Granon2***	14	44.97	6.63	2230	0.645	0.348	0.733	8	1734–1993	222	0.339	0.3	0.6
HautGarreton**	15	44.21	6.73	1900	1.568	0.981	0.779	10	1824–1981	144	0.419	0.3	0.6
Infernet**	16	44.51	6.70	2100	1.200	0.547	0.725	18	1654–1986	248	0.339	0.2	0.5
Izoard***	17	44.84	6.73	2150	0.699	0.377	0.783	12	1734–1993	229	0.291	0.3	0.8
Karellis****	18	45.22	6.40	1650	1.560	0.749	0.861	5	1755–1983	162	0.383	0.2	0.5
LaColle**	19	44.18	6.72	1800	1.956	1.065	0.718	10	1732–1981	153	0.393	0.3	0.4
LaRepose****	20	45.20	6.73	1790	1.004	0.477	0.812	10	1700–1983	214	0.299	0.2	0.7
Lavancher*	21	45.96	6.89	1750	1.947	0.912	0.751	20	1775–1994	125	0.336	0.3	0.4
LeBesseil****	22	45.21	6.73	1450	1.081	0.541	0.728	10	1732–1983	190	0.250	0.3	0.6
LeBochet****	23	45.24	6.40	1050	1.214	0.799	0.832	10	1791–1984	145	0.315	0.3	0.5
LeJeu***	24	45.23	6.81	2000	0.877	0.399	0.805	12	1665–1994	191	0.338	0.2	0.6
LesBans**	25	44.92	6.70	2000	0.701	0.347	0.713	13	1640–1995	270	0.212	0.3	0.7
LesClots**	26	44.82	6.47	2100	1.354	0.614	0.654	15	1748–1995	192	0.306	0.3	0.7
Melezet*	27	44.87	6.63	2150	1.168	0.557	0.792	13	1752–1995	189	0.282	0.2	0.6
Merveilles****	28	44.05	7.45	2200	0.353	0.142	0.560	37	933–1974	486	–0.007	0.3	0.6
Morgon**	29	44.49	6.42	1930	0.974	0.536	0.777	18	1679–1989	262	0.290	0.3	0.7
Moulins****	30	45.23	6.41	1400	0.865	0.736	0.828	5	1830–1983	149	–0.021	0.3	0.7
Moutieres*	31	44.30	6.82	2150	0.706	0.359	0.737	17	1414–1995	405	0.154	0.3	0.7
Orgeres****	32	45.22	6.68	2100	1.003	0.474	0.771	26	1353–1973	319	0.163	0.2	0.5
Oriol*	33	44.80	6.60	2180	0.618	0.347	0.762	19	1381–1989	447	0.217	0.3	0.7
PasArchais**	34	44.16	6.36	1600	2.576	1.164	0.645	11	1815–1989	72	0.195	0.3	0.6
PuyStAndre**	35	44.89	6.56	2300	0.609	0.310	0.811	14	1651–1994	275	0.134	0.2	0.6
Roche1**	36	44.68	6.80	2100	1.098	0.494	0.682	14	1782–1989	178	0.374	0.3	0.7
Roche2**	37	44.68	6.80	2100	0.593	0.352	0.779	12	1617–1990	253	0.260	0.3	0.6
Salese**	38	44.15	7.24	2150	1.122	0.679	0.761	17	1701–1980	238	0.134	0.3	0.6
Souliers******	39	44.48	4.46	2250	0.808	0.421	0.734	14	1448–2009	308	0.365	0.3	0.7
StJacques***	40	45.53	6.70	1990	0.971	0.372	0.623	12	1737–1993	173	0.241	0.3	0.6
Tourmentier****	41	45.27	6.41	1450	0.882	0.627	0.855	5	1784–1983	183	0.149	0.3	0.5
Tournoux1**	42	44.47	6.74	2000	1.027	0.644	0.757	6	1747–1990	182	0.348	0.3	0.6
Tournoux2**	43	44.47	6.74	2000	1.139	0.524	0.734	10	1724–1990	221	0.170	0.2	0.6
Tourtourel**	44	44.32	6.44	1820	1.331	0.650	0.685	19	1728–1989	195	0.262	0.3	0.6

Note: The chronology statistics include mean ring width (MRW), standard deviation (SD), and first-order serial autocorrelation (AC) computed on the raw tree ring series; and first-order serial autocorrelation (AC b.s.), mean sensitivity (MS), and mean interseries correlation (r_{bt}) computed on the indexed tree ring series. Sources (published or not) for the original larch chronology: *, J.-L. Edouard; **, F. Guibal; ***, V. Petitcolas; ****, L. Tessier; *****, C. Belingard; ******, M. Saulnier.

et al. 2006). However, the density of the LBM pine populations is always considerably lower, peaking at 60–100 shoots infested per pine, while larch populations peak at ca. 400–800 larvae·kg^{-1} of foliage, i.e., more than 50 000 individuals per tree (Dormont et al. 2006). Thus, variations in the width of pine tree rings due to LBM outbreaks were considered negligible. In a study carried out in the Susa Valley (Italian Alps), Nola et al. (2006) confirmed that LBM did not play an important role in shaping stone pine growth rate. Therefore, we used regional chronologies of stone pine as reference chronologies, each corresponding to several local stone pine chronologies grouped according to their specific latitudinal climatic response (Saulnier et al. 2011). The use of regional chronologies can minimize the effect of nonclimatic factors and enhance the common climatic signal (Fritts 1976; Carrer 2011). The climatic variations in the host index series were removed through subtraction of the non-host index series in accordance with the strategy developed by Nash et al. (1975) and extended to insect outbreak investigation by Swetnam et al. (1985).

Thus an episode of LBM outbreak was identified when both (*i*) indexed larch chronologies recorded an abrupt decrease in growth (Fig. 2), i.e., a standard deviation lower than –1, and (*ii*) the difference between indexed chronologies of stone pine and larch was higher than 1.5. This double check prevents mistakes in the identification of LBM outbreaks such as those occurring during an extremely cold year leading to a strong growth rate decrease for the two species.

Because LBM outbreak identification, resulting from a double requirement, is a qualitative variable, we used the percentage of population detecting a LBM outbreak to study the long-term reconstruction at the alpine scale and an index corresponding to the value recorded by the population (indexed tree ring difference between stone pine and larch) to perform analysis at a more local

scale. These results were used to measure the intensity of the LBM events at different scales to perform the following analyses:

- intensity at the regional or alpine scale, expressed in percentage of the populations showing a LBM outbreak, allowing discussion of the temporal patterns and long-term history of the LBM outbreaks;
- intensity at the population scale, expressed as the difference between the larch and stone pine index chronologies, to be used for investigating the spatial pattern of the LBM outbreaks.

Spatial pattern analyses

We applied a principal component analysis (PCA; Jolliffe 2002) as a clustering technique to explore and elucidate a spatial pattern of LBM outbreaks through the French Alps. This enabled common features to be identified and specific relevant local characteristics to be detected (Richman 1986). The aim of the PCA is to reduce the size of large databases by transforming the multitude of correlated variables that compose them into new independent variables called principal components. These key components retained all of the information carried by the input data while reducing redundancy. They were calculated on the variable covariance matrix. We decided to retain only the components that expressed at least 5% of the variability of the original variables, a criterion previously used in similar dendroecological studies (Peterson et al. 2002; Case and Peterson 2005; Carrer et al. 2007).

The PCA was computed on the indices matrix (i.e., the intensity at the population scale in the "LBM reconstruction" section) corresponding to the tree ring growth difference between stone pine and larch for the period common to all populations (1830–1961). Scatterplots of the weighting coefficients for the first two PCs displayed the clustering of the variables with similar modes.

Temporal pattern analyses

To study the temporal continuity of the LBM events throughout the French Alps, we performed temporal analyses on the reconstruction of LBM outbreaks for the whole of the French Alps. The spectral (or correlation) techniques make the assumption that the statistical properties of the time series do not vary with time, i.e., are stationary. However, ecological processes typically violate the stationarity assumption and there are increasing numbers of papers that underline the nonstationary features of population dynamics (Cazelles and Hales 2006).

We applied a complex continuous wavelet transform (CCWT) to assess a linear and local time–frequency (or time scale) analysis and the characterization of the spectral evolution of the signal (Grossmann et al. 1989; Lau and Weng 1995; Torrence and Compo 1998; Cazelles et al. 2008). The dilation property of the transformation gives a local and multiscale analysis of transient phenomena that linear classical time–frequency methods do not allow (Grossmann and Morlet 1984; Saracco 1994). This transformation makes it possible to decompose an arbitrary signal into elementary contributions of functions called wavelets obtained by dilation "a" in time and translation "τ" in time of a "mother wavelet" or analyzing wavelet $\psi(t)$. $\psi(t)$ is used as a band-pass filter to the time data that are treated as a signal (Grinsted et al. 2004; Setz 2011).

The analyzing wavelet $\psi(t)$ can be either real or complex. Here, we use the Morlet wavelet (a complex function), which is well localized both in time and frequency domains (eqs. 2 and 3). Two complementary information items from the CCWT are then obtained: the modulus $|W_x(\tau, a)|$ and the phase $\mathrm{Arg}[W_x(\tau, a)]$ (Grossmann and Morlet 1984) (note that if the analyzing wavelet ψ is real, the wavelet transform will be real).

From the phase of the transform, we can extract a set of ridges or spectral lines corresponding to frequency modulation laws of arbitrary signals, with respect to the analyzing or mother wavelet, while the values of modulus along these ridges provide amplitude modulation laws (Saracco et al. 1991). From the isometry property of the transform, the square modulus (eq. 5) of the wavelet coefficients can be interpreted as a density of energy in the time-scale half-plane (Valero and Saracco 2005; Saracco et al. 2009). Let $\psi(t)$ be the analyzing wavelet or "mother wavelet":

$$\psi(t) = \pi^{-1/4} e^{(-i2\pi f_0 t)} e^{(-t^2/2)} \tag{1}$$

The wavelets family generated by dilation "a" and translation "τ" of the mother wavelet $\psi(t)$ is, with the norm L_2,

$$\psi_{\tau,a}(t) = \frac{1}{\sqrt{a}} \psi\left(\frac{t-\tau}{a}\right) \tag{2}$$

The wavelet coefficient of the CCWT at a point (τ, a) is defined by the scalar product of the time series $x(t)$ with the wavelet family $\psi_{t,a}(t)$:

$$\begin{aligned} W_x(\tau, a) &= \frac{1}{\sqrt{a}} \int_{-\infty}^{+\infty} x(t) \psi^*\left(\frac{t-\tau}{a}\right) \mathrm{d}t \\ W_x(\tau, a) &= \int_{-\infty}^{+\infty} x(t) \psi^*_{\tau,a}(t) \mathrm{d}t \end{aligned} \tag{3}$$

where ψ^* is to the complex conjugate of ψ. The parameter "a" is the dilation ($a > 1$) or contraction ($a < 1$) factor of the analyzing wavelet $\psi(t)$, corresponding to different scales of observation. The parameter "τ" can be interpreted as a temporal translation or shift of the function $\psi(t)$, which allows the study of the signal $x(t)$ locally around the time t.

The choice of the analyzing wavelet is free, but it has to verify the admissibility condition deduced from the isometric property of the transform in the following sense (Saracco 1994): there exists for every $x(t)$ a constant C_g depending only on the wavelet ψ such that

$$\begin{aligned} x(t) &= \frac{1}{C_g} \int_{-\infty}^{+\infty} \int_0^{\infty} \frac{1}{a^2} W_x(\tau, a) \psi_{\tau,a}(t) \mathrm{d}\tau \mathrm{d}a \\ \text{where } C_g &= \int_0^{\infty} \frac{\|\hat{\psi}(f)\|^2}{f} \mathrm{d}f \end{aligned} \tag{4}$$

and $\hat{\psi}(f)$ is the Fourier transform of $\psi(t)$. By analogy with the Fourier analysis, the wavelet power spectrum $S_x(\tau, f)$ of the continuous signal $x(t)$ is defined as

$$S_x(\tau, f) = \|W_x(\tau, f)\|^2 \tag{5}$$

This wavelet spectrum can also be averaged in time (eq. 7), referred to as the global averaged wavelet power spectrum (Torrence and Compo 1998), allowing the determination of the characteristic scales.

$$S_x(f) = \frac{\sigma_x^2}{T} \int_0^T \|W_x(\tau, f)\|^2 \mathrm{d}\tau \tag{6}$$

This analysis makes it possible to detect the presence of cycles and the temporal evolution of the period of the oscillations.

As in Fourier analysis, the wavelet power spectrum can be extended to quantify statistical relationships between two time series

$x(t)$ and $y(t)$. The wavelet cross-spectrum provides local information on the covariance of both time series at particular frequencies. However, previous studies have pointed out that wavelet cross-spectrum appears poorly suited for interpretation of the interrelation between two nonstationary processes and recommend the introduction and use of wavelet coherence analysis (Maraun and Kurths 2004; Cazelles et al. 2008; Labat 2010). The wavelet coherency is defined as the cross-spectrum normalized by the spectrum of each signal (Cazelles et al. 2008):

$$(7) \qquad R_{x,y}(\tau, f) = \frac{\|\langle W_{x,y}(\tau, f)\rangle\|}{\|\langle W_{x,x}(\tau, f)\rangle\|^{1/2} \|\langle W_{y,y}(\tau, f)\rangle\|^{1/2}}$$

The notion of coherency in signal processing consists, from a general point of view, of a normalized measure of the correlation or "degree of likeness" from 0 to 1 between two arbitrary signals. Thanks to the dilation property of the wavelet transforms, we can detect local information about where these signals are linearly correlated and define a particular and temporal location in the time-scale (time–frequency) half-plane. This analysis is particularly suitable for studying the potential effects of climate, particularly temperature, on LBM outbreaks.

Climate data

The climate model used in this analysis was developed by Büntgen et al. (2005). This model consists of a June–August temperature reconstruction based on tree rings from both living trees and relict woods from the Alps. Larch data from four Alpine valleys in Switzerland and pine data from the western Austrian Alps, both located above 1500 m a.s.l., were used is this reconstruction.

Results

Statistical parameters (Table 1)

The estimated mean tree age per site (at coring height) of the 620 analyzed larch trees varies from 72 to 486 years. Mean sensitivity and first-order serial autocorrelation range from 0.2 to 0.3 and from 0.56 to 0.86, respectively. High first-order autocorrelation indicates that the radial growth throughout the network is strongly influenced by the conditions prevailing in the preceding year and by the geometrical effect of increasing stem circumference. The mean autocorrelation decreases from 0.74 to 0.28 after detrending, which evidences the efficiency of the double-detrending process. A particularly useful parameter for assessing the chronology quality is the interseries correlation (r_{bt}), which varies from 0.4 to 0.8. EPS value varies from 0.84 to 0.98, which indicates a high common signal between series, suggesting that the high variability of r_{bt} may reflect a high individual variability.

LBM outbreak events

Years of LBM outbreak were detected in each population. Table 2 summarizes the characteristics of the LBM events for all the populations. The French Alps chronology corresponds to the percentage of populations with LBM outbreaks by year. A wide disparity is observed between populations. To compare the results, the number of outbreaks (Nb) is expressed as the number of outbreak events per century (Nb/century) (Table 2). On average, six outbreaks affect the larch populations per century, with a minimum of two (Merveilles) and a maximum of 11 (Fres1B). The recurrence interval between two outbreaks is, on average, about 20 years and is characterized by strong variability, with a minimum of 2 years observed for several populations and a maximum of 240 years observed for the population of Beauvezer1.

LBM reconstruction in the French Alps during the last half-millenium revealed regular cyclic fluctuations of the phenomena with peak periods of 1–2 years immediately followed by declining phases (Figs. 3A and 3B). This characteristic is common to all populations throughout the French Alps. The average time calculated between two outbreak peaks is 7.6 years.

Multispatial gradient

Principal component analysis (PCA) was used as a clustering technique to test groups with similar LBM outbreak years and to elucidate a spatial pattern of LBM outbreaks. Results of PCA applied on the LBM intensity matrix at the local scale (cf. methods, i.e., the matrix in which data for each larch population correspond to the tree ring growth difference between stone pine and larch) show that the two first axes explained 20% and 14% of the total inertia, respectively (Fig. 4). Weighting coefficients obtained were then correlated to some environmental variables. The correlation between PC1 scores and site elevation is 0.64 and between PC2 scores and site latitude is 0.69 ($p < 0.05$). The obvious site distribution along a diagonal in the scatterplots suggests that both PCs contribute to the characterization of the site-specific LBM outbreak events. Low-elevation chronologies present negative scores on the first axis, whereas in the positive direction, the main structuring populations are located above 1500 m a.s.l., thus illustrating two different patterns of LBM outbreak events (Fig. 4A).

With regard to the latitudinal gradient, PC2 clearly differentiates sites located in the northern French Alps in the positive direction from clusters of chronologies located in the central and southeastern parts of the French Alps (Fig. 4B). These results yield significant heterogeneity in the spatial pattern, providing a basis for distinguishing outbreak events according to elevation and latitude of the populations.

As a consequence, on the basis of a latitudinal gradient, three LBM outbreak chronologies have been reconstructed:

- the northern group, including populations located in the Tarentaise Valley and in the Maurienne Massif;
- the intermediate group, including populations located in the Briançon and the Embrun valleys and in the Queyras Massif;
- the southern group, including populations located in the Ubaye Valley and in the Mercantour Massif.

The cross-correlations between the three chronologies show that both the southern and northern populations are lagging 1 year behind the intermediate populations (Figs. 5A and 5B), while the southern and northern populations have maximum correlation for a time lag of 0 (Fig. 5C).

Temporal heterogeneity

The reconstruction and wavelet analysis performed on the three regional chronologies is shown in Fig. 6 for the common period 1551–1994. It reveals the existence of 8-year cycles in each cluster with more or less continuity in the signal. The intermediate group presents the longer continuous signal. For the northern group, this signal extends less continuously over the period from 1550 to 1700. Within the southern group, the cycles were particularly strong between 1600 and 1650 and since 1930.

The wavelet analysis was applied on the LBM reconstruction throughout the French Alps, expressed as the percentage of populations with LBM events over the full reconstruction period, i.e., between 1500 and 2003. Results are presented according to the modulus and the phase of wavelet coefficients. Wavelet analysis in the LBM data reveals the presence of a strong power spectrum on the modulus around 8-year periodicities (Fig. 7A) and thus confirmed on the phase with significant 4 and 8–12 year periodicities (Figs. 7B and 7C; only the ridge around 8–12 years is represented in Fig. 7B). These periodicities mirror almost exactly the well-known LBM cycle. Both cycles are present throughout the entire 1500–2003 time series, with the exception of a loss of power from 1690 to 1790, especially between 1700–1740 and 1750–1800, and since the early

Table 2. Characteristics of the LBM outbreaks for each the populations according to (*i*) the number of outbreaks identified in chronologies expressed as the total number (Nb) and the average number per century (Nb/century) and (*ii*) interval between two outbreaks expressed as the mean, the minimum, and the maximum number of years.

			LBM outbreaks				
					Interval between LBM outbreaks, years		
Population	Time period	MTA	Nb	Nb/century	Mean	Minimum	Maximum
Beauve2	1421–1993	355	12	3.38	46.78	3.00	240.00
Beauve4	1160–1994	835	21	2.51	21.67	4.00	47.00
Bellec	1812–1993	182	7	3.85	22.33	2.00	69.00
Braiss	1417–1995	579	28	4.84	19.83	5.00	79.00
Chardo	1492–1989	948	27	2.85	21.82	4.00	59.00
Clap	1557–1995	439	23	5.24	19.47	7.00	52.00
Echalp	1338–1995	658	58	8.81	10.17	2.00	28.00
Fouill	1669–1981	313	20	6.39	16.07	2.00	104.00
Fres1A	1632–1990	359	27	7.52	12.56	5.00	34.00
Fres1B	1542–1961	420	45	10.71	9.83	5.00	27.00
Fres2	1474–1992	519	32	6.17	19.44	7.00	36.00
Gordol	1830–1983	154	10	6.49	19.14	8.00	35.00
Gra	1710–1993	284	23	8.10	20.73	7.00	58.00
Gra2	1734–1993	260	16	6.15	20.50	2.00	69.00
HautGa	1824–1981	158	9	5.70	29.20	9.00	68.00
Inf	1654–1986	333	14	4.20	26.00	4.00	96.00
Izoard	1734–1993	260	21	8.08	15.64	7.00	39.00
Karell	1755–1983	229	15	6.55	22.00	3.00	74.00
LaColl	1732–1981	250	24	9.60	20.09	9.00	62.00
LaRepo	1700–1983	284	19	6.69	22.36	2.00	91.00
Lavanc	1775–1994	220	14	6.36	24.50	5.00	52.00
LeBess	1732–1983	252	20	7.94	23.78	2.00	76.00
LeBoch	1791–1984	194	15	7.73	12.36	3.00	39.00
LeJeu.	1665–1994	330	19	5.76	28.00	6.00	103.00
LesBans	1640–1995	356	19	5.34	20.93	3.00	91.00
LesClots	1748–1995	248	21	8.47	13.53	7.00	29.00
Melezet	1752–1995	244	12	4.92	30.71	7.00	59.00
Mervei	933–1974	1042	21	2.02	22.76	3.00	74.00
Morgon	1679–1989	311	20	6.43	29.44	7.00	61.00
Moulin	1830–1983	154	11	7.14	11.70	6.00	20.00
Moutie	1414–1995	582	32	5.50	16.11	6.00	43.00
Orgere	1353–1973	621	22	3.54	21.11	6.00	115.00
Oriol	1381–1989	609	45	7.39	20.11	3.00	51.00
Pas_Ar	1815–1989	175	6	3.43	25.80	3.00	67.00
PuyStA	1651–1994	344	20	5.81	21.85	2.00	69.00
Roche1	1782–1989	208	16	7.69	16.09	6.00	44.00
Roche2	1617–1990	374	26	6.95	16.61	2.00	44.00
Salese	1701–1980	280	17	6.07	20.83	7.00	79.00
Soul	1448–2009	562	33	5.87	17.33	5.00	54.00
StJacq	1737–1993	257	16	6.23	16.25	4.00	65.00
Tourme	1784–1983	200	12	6.00	19.33	4.00	62.00
Tourn1	1747–1990	244	22	9.02	11.35	6.00	26.00
Tourn2	1724–1990	267	14	5.24	23.50	8.00	51.00
Tourto	1728–1989	262	14	5.34	17.58	2.00	42.00
Total	Mean		20.86	6.14	20.39	4.77	63.25
	Minimum		6	2.02	9.83	2.00	20.00
	Maximum		58	10.71	46.78	9.00	240.00

1980s (Figs. 7A and 7B). Regarding the wavelet analysis of climate reconstruction data for the same 1500–2003 time period (Figs. 7D–7F), the modulus and the phase of the wavelet analysis show the existence of several continuous periodic signals for different periods. The signal that appears closest to a continuous periodic signal is found for 2–4 and 8–12 year periods, and more locally for the 45–64 year periods. The abrupt change, characterized by a loss of significant power spectrum in LBM wavelet analysis observed between 1690 and 1790 (Figs. 7A and 7B), follows the increasing power spectrum of the 8–12 year periodic signal (discontinuous; Fig. 7D) in climate series and coincides with a change in the ridge around 8–12 years (highlighted by white lines in Fig. 7E), which represents the frequency modulation laws extracted on the phases of CCWT.

This striking link between the LBM data and climate reconstruction around those same 8–12 year periodicities is supported by the strong and almost continuous coherence (Fig. 8A) and the phase coincidence (Figs. 8B, 8C, and 8D). The modulus of the wavelet coherency analysis clearly shows a strong component, i.e., a high amplitude of the signals, near 1 around the 8-year periodicity, especially around 1500, 1590, 1690, 1740, and 1790 and since 1950. The magnitude of the component increases and decreases over time but is generally strong. Furthermore, for these periods, Figure 8D reveals phase coinci-

Fig. 3. (A) Histogram of the French Alps LBM outbreaks chronology expressed as the percentage of the larch populations with LBM for the period 1500–2000. The dashed line represents the total number of larch populations. (B) The fitted curve of French Alps LBM outbreaks chronology using running average.

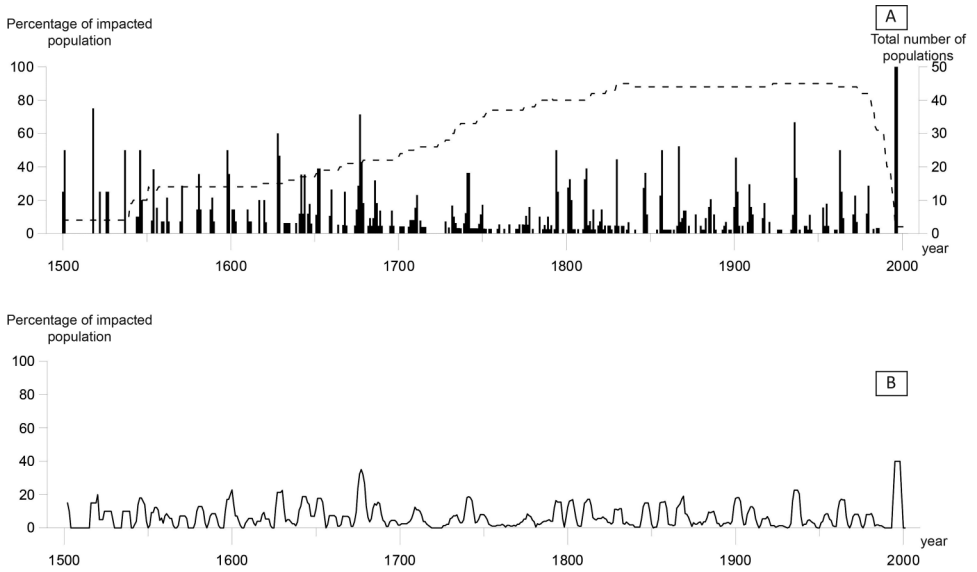

Fig. 4. Scatterplots of the relationships between (A) site elevation with weighting coefficients for PC1 and (B) site latitude with weighting coefficients for PC2. Axis labels report the percentage of variance expressed by each component. Labelled numbers refer to Table 1.

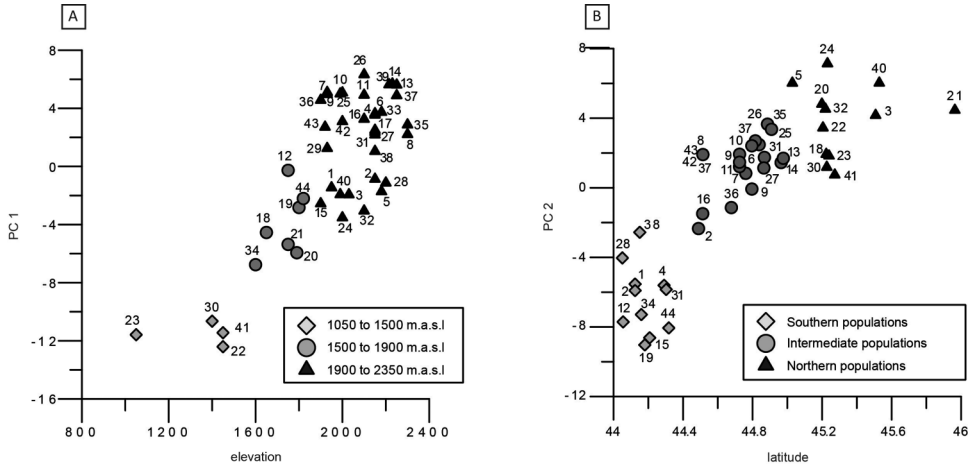

dences between the CCWT of both climate data and the strong periodic LBM outbreaks. Figures 8B and 8C, which represents the unwrapped phases for a period of around 8 years, confirms that both LBM and climate signals follow the same cyclicity (same frequency modulation laws, white lines) throughout time. Focusing on the years with a strong component of coherency (white-outlined rectangle), phase lines (vertical lines) appear either larger (1590–1620; 1640–1660; 1680–1720; 1740–1780; 1940–2000), with a ridge located at higher frequency, or narrower (1880–1940). The loss of power identified on the two components of CCWT of LBM (1700–1740 and 1750–1800, and since the early 1980s) corresponds to the low power of the coherence and to the slight phase difference between LBM and climate (Figs. 8B and 8C). The phase difference varies between $1/3\pi$ and π, which evidences that LBM is lagging approximately 3–6 years behind climate (Fig. 8E).

Results from both modulus and phases show that the dynamics of LBM outbreaks are very closely associated with climate. When a change in the climate signals occurs, the modulus of CCWT of LBM shows a lower amplitude (density of energy) or a higher amplitude, but frequency modulation laws extracted in the phase continue to follow closely those of climate.

Discussion

Evidence of an epicenter within the French Alps

The optimum 1700–2000 m a.s.l distribution zone for LBM outbreak probably explains the pattern of results observed on PC1, closely and significantly correlated to the elevation (Baltensweiler and Fischlin 1988). The populations at both low and very high elevations, i.e., located on the margins of this optimum distribution range, present a less marked cyclicity and show less marked evidence of epidemics. It cannot be excluded that past outbreaks of some other defoliator insect known to attack larch such as the Nun moth (*Lymantria monacha* L.) may have generated a tree ring signal similar to that of the LBM. However, contemporary observations from 1950 onwards reveal only very scattered outbreaks of species other than LBM in the Alps (i.e., a local episode of Nun moth outbreak in the Briançon area during 1985 and an outbreak of the larch sawfly (*Cephalcia* sp.) in the southern part of the French Alps during 2011–2012). Thus species other than LBM likely had a very limited effect on larch tree rings.

The relationship between latitude and the occurrence of LBM episodes illustrates the presence of “travelling waves” associated

Fig. 5. Cross-correlation between (A) the northern and intermediate populations, (B) the southern and intermediate populations, and (C) the northern and southern populations. CCF corresponds to the cross-correlation between $x(t + k)$ and $y(t)$. In parts A and B, we used intermediate populations as the reference, so time lag identified corresponds to the lag or advance of LBM in the northern population (A) and in the southern population (B). In part C, we used the northern population as reference.

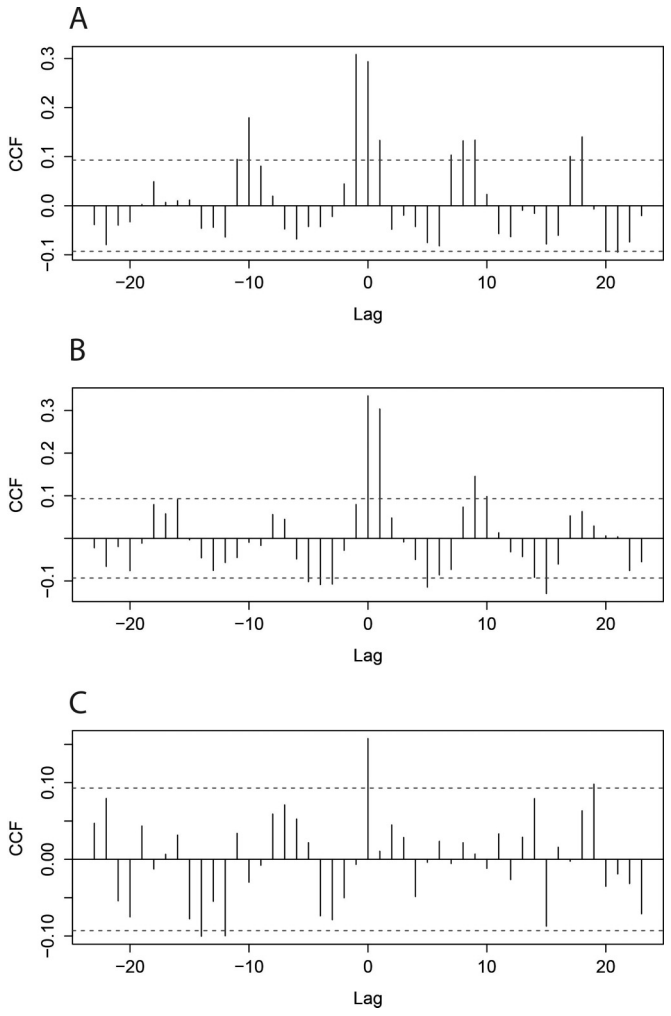

with epicenter zones located in the intermediate subalpine French Alps, as already suggested in other studies (Bjørnstad et al. 2002; Johnson et al. 2004; Delamaire 2009) (see Supplementary material[1] and Fig. 5). Bjørnstad et al. (2002) demonstrated that spatial gradients in habitat quality (reflected in LBM population growth rate) or advective (directional) dispersal can result in recurring directional waves. In contrast, Johnson et al. (2004) supported an alternative hypothesis based on habitat geometry suggesting that habitat connectivity plays a key role in shaping spatial dynamics and, in particular, epicenter dynamics in the LBM. In general, three possible spatial patterns can emerge in cyclic population dynamics: (*i*) spatial synchrony, (*ii*) spatial asynchrony, and (*iii*) travelling waves.

Our results tend to confirm the hypothesis that the epidemics start in the intermediate subalpine zone of the French Alps before spreading north and south during the following years (phenomena illustrated in the video in Supplementary material[1]). We used cross-wavelet analysis to evidence a link between the starting points of the LBM outbreaks within the three population groups. The travelling waves are typified by population in partial synchrony with a time lag. The wavelet analysis clearly shows that the usual functioning of the LBM cycle is only found in the inner Alps. In the northern and southern Alps, the continuity of the signal for a period of about 8 years appeared more sporadic and variable periodicity is likely.

It would be of prime interest to link the spatial pattern observed in the French Alps with those obtained in others areas in the Alps, especially in Switzerland. Indeed, Johnson et al. (2004) defined a major epicenter in France, located in the Briançon area (southwestern Alps), and a minor one in Switzerland, situated in the Engadine (central Alps). Both epicenters are located in zones with the highest concentration of closely connected favorable habitats. Johnson et al. (2004) suggested that the mosaic arrangement of the landscape is responsible for initiating travelling waves.

The spread and the intensity of the attacks was not uniform throughout the alpine area, being greater in the western Alps than in the eastern Alps (Baltensweiler and Rubli 1999; Bjørnstad et al. 2002; Nola et al. 2006) and in the continental valleys as compared with the valleys with a more oceanic climate. As already suggested by Delamaire (2009), it is highly likely that the major epicenter in the Briançon region is involved in protecting and dispersing genetic diversity during the outbreaks and plays a major role for migrations in the spatiotemporal dynamics of the populations. In fact, by acting as a homogenizing factor in genetic diversity and as an active component of the spatial development of the outbreaks (i.e., "travelling waves"), LBM dispersal shapes the genetic pattern observed today in the outbreak areas of LBM (Delamaire 2009).

Abrupt shift in LBM events linked to climate change

The chronology of LBM epidemics reconstructed for the whole of the French Alps showed changes over time in terms of both intensity and frequency. Thus, an abrupt change was observed during the period 1690–1790. Prior and subsequent to this period, LBM outbreaks were characterized by a cyclicity of about 8 years, as widely described in the literature (Baltensweiler et al. 1977; Baltensweiler and Fischlin 1988; Dormont et al. 2006; Esper et al. 2007; Büntgen et al. 2009; Delamaire 2009; Delamaire et al. 2010). This change, common to the three population groups, was analyzed over extended varying periods of time and may be attributed to, at least to some extent, a temperature change as revealed by coherency analysis performed on the LBM time series and climate reconstruction (Büntgen et al. 2005). Johnson et al. (2010) suggested an upward shift in the elevational optimum due to climatic warming. These rapid changes in the climate and in the zone of potential distribution of certain taxonomic groups have been reported in a number of other studies (Johnson et al. 2010; Maggini et al. 2011; Roques 2015). By inference from the theoretical model developed by Maggini et al. (2011), it is possible to hypothesize that fluctuations in the distribution of LBM have occurred during the last 400 years, which explains the cyclical nonlinearity during this period. The onset of the 18th century saw the start of a general temperature drop (Little Ice Age) in Europe and North America. This temperature drop is clearly visible in the tree rings, as demonstrated in a number of climatic reconstruction studies (Büntgen et al. 2006; Corona et al. 2011).

During the Little Ice Age, a decrease of sunspots resulted in the coldest period, known as the Maunder Minimum. The temperature decrease probably caused an ecophysiological response in the trees, in particular, a later budburst, which may have resulted in

Fig. 6. Power spectrum of the complex continuous wavelet transform (CCWT) of the French Alps LBM outbreaks: (A) northern populations, (B) intermediate populations, and (C) southern populations. The 95% significance level against red noise is shown as a black contour. The thick black contour designates the 5% significance level against red noise, and the cone of influence where edge effects might distort the picture is shown as more lightly shaded time–frequency values for the wavelet power. [Colour online.]

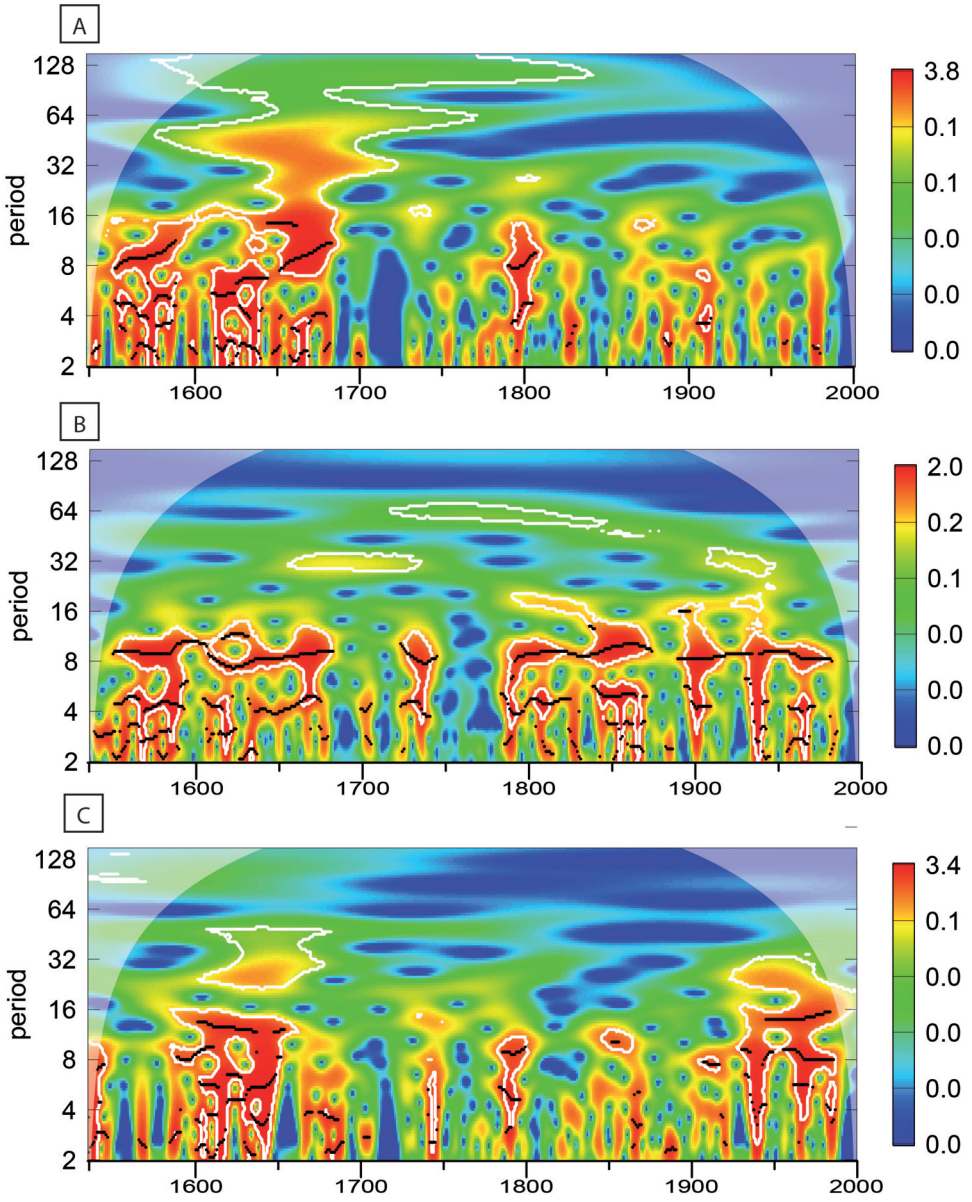

a desynchronization of LBM egg hatching from the foliage appearance in previously optimum elevational zones. It could thus explain the population "collapses" described by Baltensweiler et al. (2008). The larch populations in this study grow at an average elevation of about 1960 m a.s.l., thus at the edges of the distribution zone of the LBM in a "normal" climate. The hypothesis of a descent to a lower elevation of this distribution zone could therefore explain the disruption of the LBM periodic signal during the 18th century (Fig. 9). The outbreak years observed during this period seem to correspond to the years when the climate favored the spread of the LBM to higher elevation zones during the major outbreak years of the species (Fig. 9C). Following the return to a favorable climate, the optimum climatic condition and the distribution zone reached higher elevations. The climate change could also have affected the spread of the LBM, as shown by a recent genetic study in the French Alps (Delamaire et al. 2010). The same trend has also been suggested by the model proposed by Johnson et al. (2010), who anticipated a rise in elevation of the insect's optimum development zone. Recent monitoring of the LBM populations in the Briançon area also showed that their density was higher above 2000 m a.s.l. (Delamaire et al. 2010).

Our results tend to confirm these results. The populations in the southern and the intermediate Alps, situated at higher elevations (>2000 m a.s.l.), have experienced strong LBM outbreaks since the middle of the 20th century. The current climate change has affected the southern and intermediate Alps much more rapidly (Intergovernmental Panel on Climate Change (IPCC) 2007; Beniston 2009), which makes the high-elevation tree populations more susceptible to frequent and intense LBM attacks (Fig. 9D).

However, it seems clear that this response pattern is limited to zones favorable to larch and that, in conclusion, the climate change effects could explain the spatiotemporal variability of the LBM, despite its presence for thousands of years.

Fig. 7. Power spectrum and phase of the complex continuous wavelet transform (CCWT) of (A, B, C) LBM data and (D, E, F) the climate model. The modulus maxima are presented in parts A and D (visible as red in the online version). The square modulus of CCWT represents the wavelet power spectrum. The white lines (B, E) on the phase map represent the ridges, i.e., the frequency modulation laws of signal extracted only on the unwrapped phase around the 8–12 years continuous periodicities. High values of power spectrum appear for periodicities of (A) 8 and 4 years for LBM data and (D) 45–64, 16–20, 8–12, and around 4 and 2 years for climate model. (C, F) Wavelet power averages across time of LBM data (C) and climate data (F); the vertical axis shows the Fourier periods and the horizontal axis shows the averages. [Colour online.]

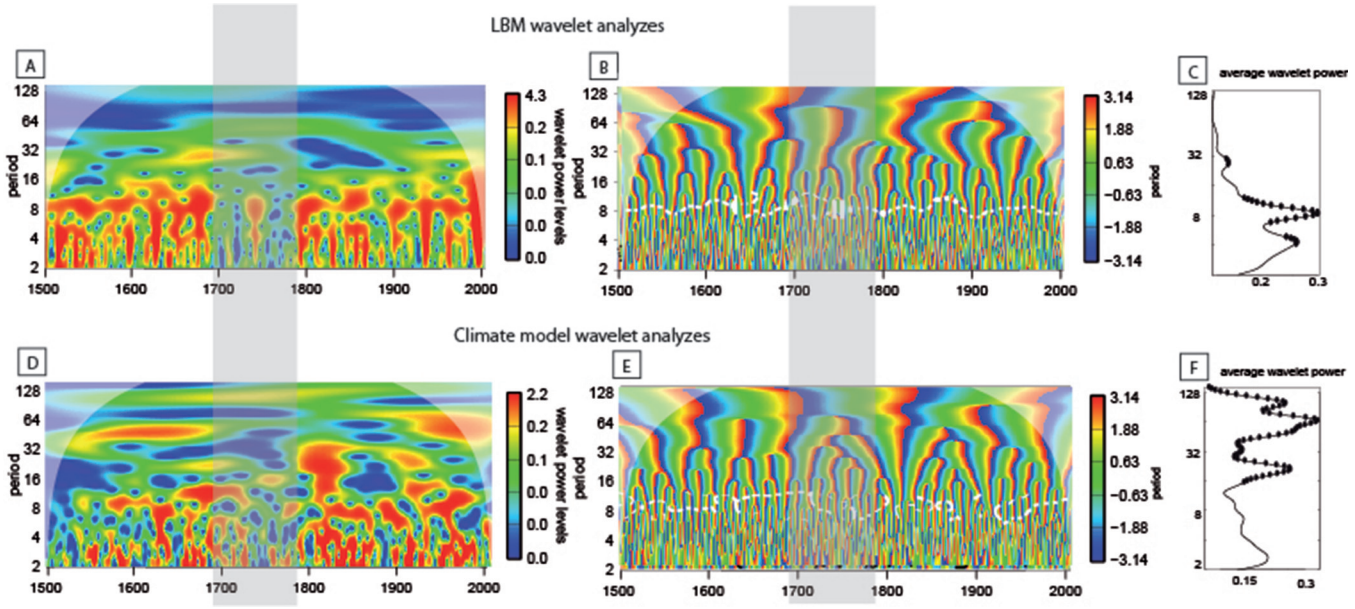

Fig. 8. (A) Coherency analyses between LBM data and the climate model for the 4–16-year period (zoom on the 8-year relevant period). The energy density maxima are presented (visible as red in the online version). (B, C) Unwrapped phase of CCWT of both LBM data (B) and climate data (C) for the 7.7–8.3 year period around the ridge (i.e., the frequency modulation laws of signals). (D) Phase difference of the wavelet transform of the two time series LBM (red line in the online version) and climate model (blue line in the online version) for the 7.7–8.3 year period. The bold dashed line displays the patterns of change in phase difference. (E) Distribution of phase differences. [Colour online.]

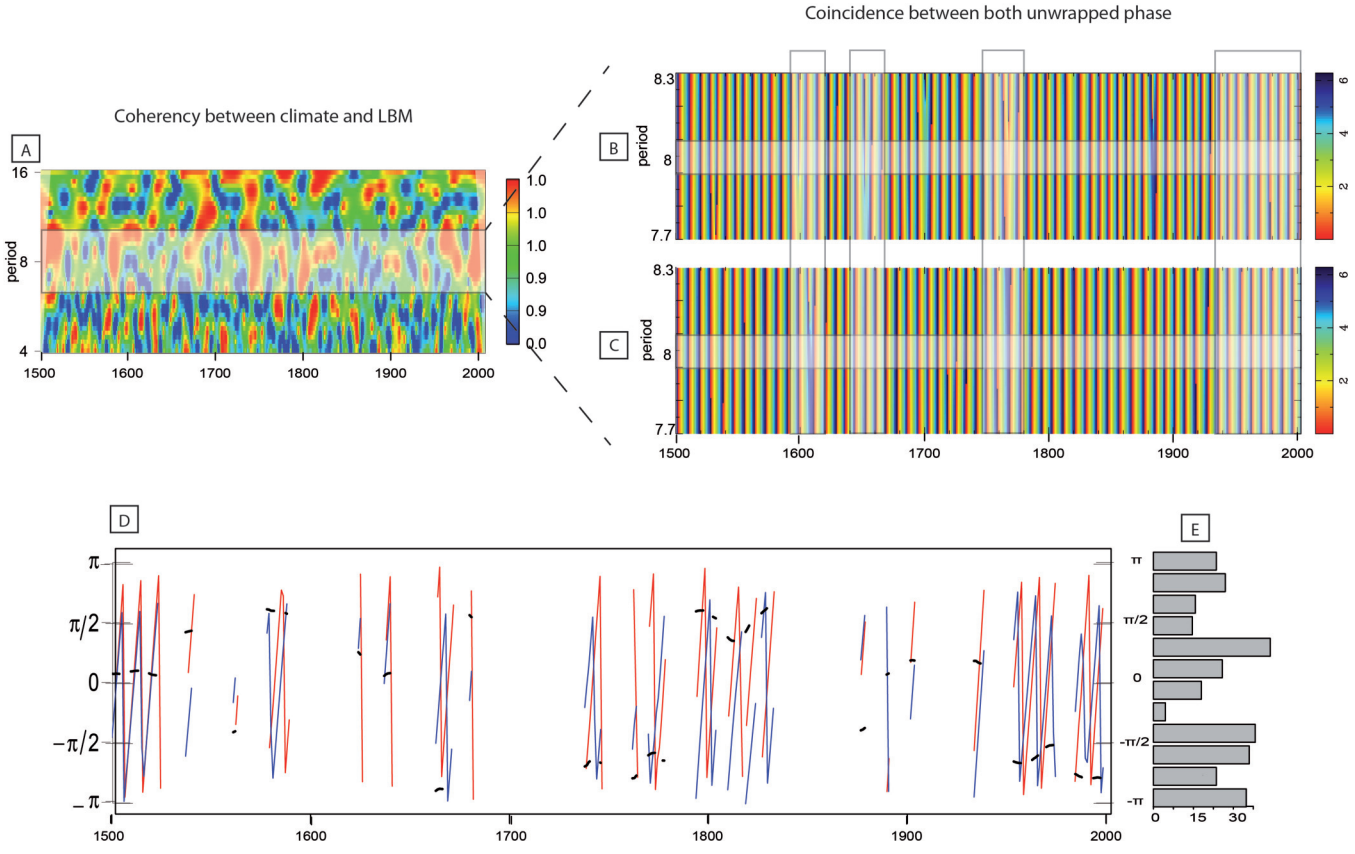

Fig. 9. (A, C, D) Reconstruction of LBM outbreaks (bar charts) (A) back to 1500, (C) for the 1690–1790 period, and (D) for the 1880–2000 period. Reconstructed June–August temperature anomalies (line charts) with respect to the 1901–2000 period. Error bars are ±1 root mean square error of the calibration periods (data from Büntgen et al. 2011). (B) Schematic illustration of LBM distribution shifts over the past 500 years in response to climate change. [Colour online.]

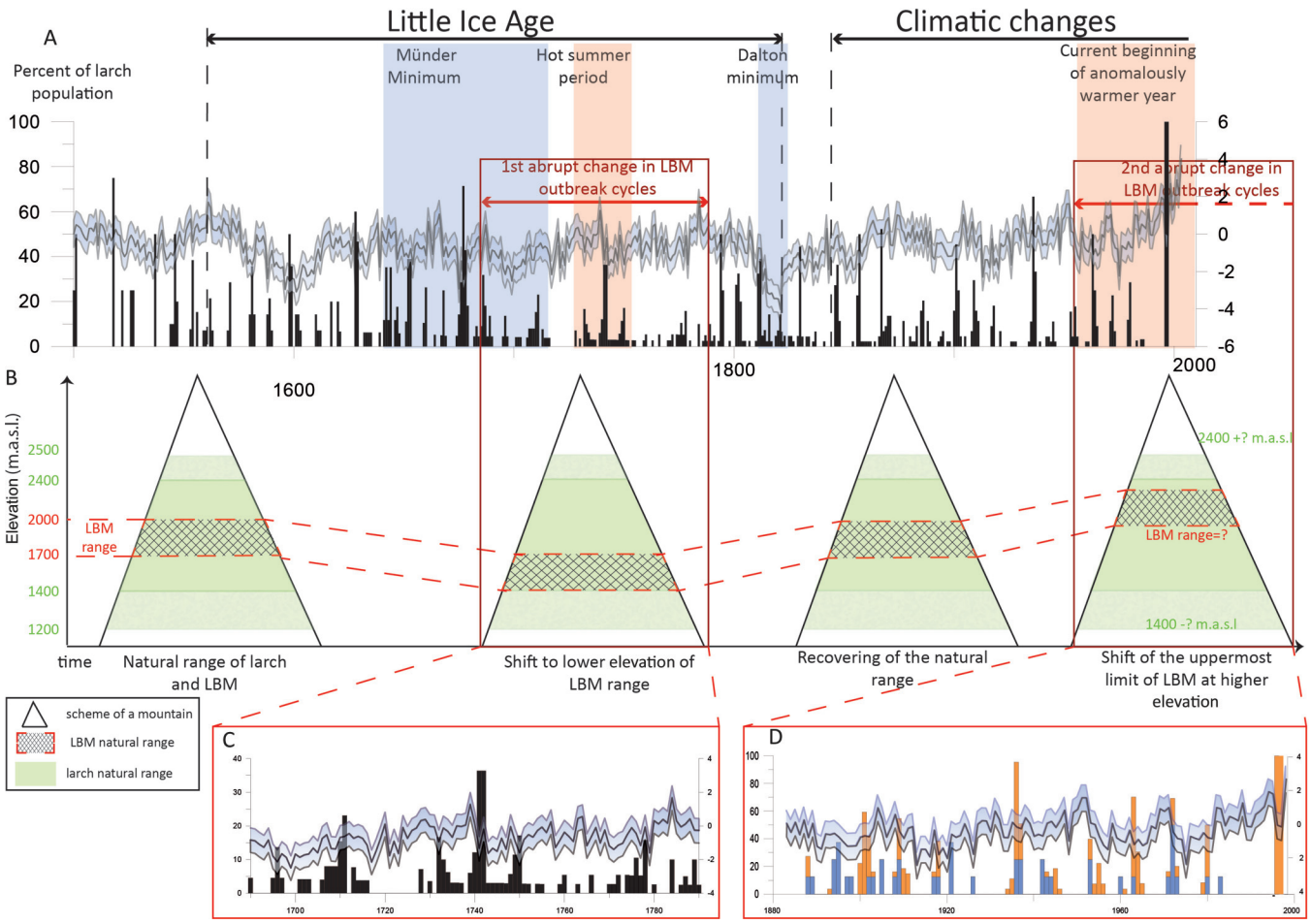

Conclusion

Understanding the cyclical dynamics of animal populations and assessing the vulnerability of such ecological systems to exogenous forcing such as climate change requires long time series of natural population variation. The long-term history of LBM outbreaks was reconstructed from tree rings of host subalpine larch in the French Alps for the period 1414–2009.

While the long persistence and regularity of LBM reoccurrence over the past 500 years in the French Alps was confirmed by this study, a pattern of spatiotemporal heterogeneity was evidenced that offers a good basis for understanding the dynamics of LBM. At the regional scale, the heterogeneity of LBM events is characterized by a 1-year delay between outbreaks occurring in the intermediate Alps and the northern and southern Alps. This asynchronism is attributed to the phenomenon of travelling waves characterized by the existence of epicenter zones from which the epidemic waves spread, similar to those observed in the European Alps (Johnson et al. 2004) and parts of the French Alps (Delamaire 2009). In this respect, intermediate populations are considered as the epicenter of the outbreak, with both a continuous signal height of a periodicity of around 8 years and usually the emergence of an epidemic 1 year before the southern and northern clusters of populations. Similarly, the periodic signal highlighted for the northern and southern TRW chronologies shows less continuity and a changing pattern over time. For all populations, a break period in the signal continuity is observed during the 18th century. Cross-wavelet analysis confirmed the role of climate in the changing patterns of LBM outbreak cycles. As several studies have already demonstrated, mountain species are expected to change their phenological rhythm and (or) their distribution in response to abrupt climate change. In consequence, the interactions between many species may be considerably altered, and thus, the ecosystem dynamics (ecological equilibrium) may be modified in unpredictable ways. On the basis of the results of this study, the LBM may be expected to shift its distribution area to higher elevations in response to warming. Such a phenomenon raises questions about the future larch forest dynamics in the French Alps according to a shift in elevation of LBM.

Acknowledgements

The collection of some tree ring chronologies used in this work was possible thanks to the European Union through the FORMAT project (contract ENV4-CT97-0641). Office National des Forêts provided sampling permission. We gratefully thank two anonymous reviewers who helped improve an earlier version of the manuscript.

References

Allstadt, A.J., Haynes, K.J., Liebhold, A.M., and Johnson, D.M. 2013. Long-term shifts in the cyclicity of outbreaks of a forest-defoliating insect. Oecologia, **172**(1): 141–151. doi:10.1007/s00442-012-2474-x. PMID:23073635.

Auer, C. 1977. Dynamik von Lärchenwicklerpopulationen längs des Alpenbogens. Mitt. Eidg. Forschungsanstalt Wald Schnee Landschaft, **53**: 70–105.

Baltensweiler, W., and Fischlin, A. 1988. The larch budmoth in the Alps. *In* Dynamics of forest insect populations: patterns, causes, implications. *Edited by* A.A. Berryman. Springer, New York. pp. 331–351. doi:10.1007/978-1-4899-0789-9_17.

Baltensweiler, W., and Rubli, D. 1999. Dispersal: an important driving force of the cyclic population dynamics of the larch budmoth, *Zeiraphera diniana* Gn. For. Snow Landsc. Res. **74**(1): 1–153.

Baltensweiler, W., Benz, G., Bovey, P., and Delucchi, V. 1977. Dynamics of larch bud moth populations. Annu. Rev. Entomol. **22**(1): 79–100. doi:10.1146/annurev.en.22.010177.000455.

Baltensweiler, W., Weber, U.M., and Cherubini, P. 2008. Tracing the influence of larch-bud-moth insect outbreaks and weather conditions on larch tree-ring growth in Engadine (Switzerland). Oikos, **117**: 161–172. doi:10.1111/j.2007.0030-1299.16117.x.

Battisti, A. 2008. Forests and climate change — lessons from insects. iForest, **1**: 1–5. doi:10.3832/ifor0210-0010001.

Battisti, A., and Larsson, S. 2015. Climate change and insect pest distribution range. *In* Climate change and insect pests. *Edited by* C. Björkman and P. Niemelä. CABI, Wallingford, UK. pp. 1–15. doi:10.1079/9781780643786.0001.

Battisti, A., Stastny, M., Netherer, S., Robinet, C., Schopf, A., Roques, A., and Larsson, S. 2005. Expansion of geographic range in the pine processionary moth caused by increased winter temperatures. Ecol. Appl. **15**: 2084–2096. doi:10.1890/04-1903.

Battisti, A., Stastny, M., Buffo, E., and Larsson, S. 2006. A rapid altitudinal range expansion in the pine processionary moth produced by the 2003 climatic anomaly. Global Change Biol. **12**: 662–671. doi:10.1111/j.1365-2486.2006.01124.x.

Beniston, M. 2009. Changements climatiques et impacts. Presses Polytechniques et Universitaires Romandes, Lausanne, Suisse.

Berryman, A.A. (*Editor*). 1988. Dynamics of forest insect populations: patterns, causes and implications. Springer, New York. doi:10.1007/978-1-4899-0789-9.

Bjørnstad, O.N., Peltonen, M., Liebhold, A.M., and Baltensweiler, W. 2002. Waves of larch budmoth outbreaks in the European Alps. Science, **298**: 1020–1023. doi:10.1126/science.1075182. PMID:12411704.

Büntgen, U., Esper, J., Frank, D.C., Nicolussi, K., and Schmidhalter, M. 2005. A 1052-year tree-ring proxy for Alpine summer temperatures. Clim. Dynam. **25**(2–3): 141–153. doi:10.1007/s00382-005-0028-1.

Büntgen, U., Frank, D.C., Nievergelt, D., and Esper, J. 2006. Summer temperature variations in the European Alps, AD 755–2004. J. Clim. **19**: 5606–5623. doi:10.1175/JCLI3917.1.

Büntgen, U., Frank, D., Liebhold, A., Johnson, D., Carrer, M., Urbinati, C., Grabner, M., Nicolussi, K., Levanic, T., and Esper, J. 2009. Three centuries of insect outbreaks across the European Alps. New Phytol. **182**: 929–941. doi:10.1111/j.1469-8137.2009.02825.x. PMID:19383093.

Büntgen, U., Tegel, W., Nicolussi, K., McCormick, M., Frank, D., Trouet, V., Kaplan, J.O., Herzig, F., Heussner, K.-U., Wanner, H., Luterbacher, J., and Esper, J. 2011. 2500 years of European climate variability and human susceptibility. Science, **331**(6017): 578–582. doi:10.1126/science.1197175. PMID:21233349.

Carrer, M. 2011. Individualistic and time-varying tree-ring growth to climate sensitivity. PLoS One, **6**(7): e22813. doi:10.1371/journal.pone.0022813. PMID:21829523.

Carrer, M., and Urbinati, C. 2004. Age-dependent tree-ring growth responses to climate in *Larix decidua* and *Pinus cembra*. Ecology, **85**(3): 730–740. doi:10.1890/02-0478.

Carrer, M., Nola, P., Edouard, J.-L., Motta, R., and Urbinati, C. 2007. Regional variability of climate–growth relationships in *Pinus cembra* high elevation forests in the Alps. J. Ecol. **95**: 1072–1083. doi:10.1111/j.1365-2745.2007.01281.x.

Case, M.J., and Peterson, D.L. 2005. Fine-scale variability in growth–climate relationships of Douglas-fir, North Cascade Range, Washington. Can. J. For. Res. **35**: 2743–2755. doi:10.1139/x05-191.

Cazelles, B., and Hales, S. 2006. Infectious diseases, climate influences, and nonstationarity. PLoS Med. **3**(8): e328. doi:10.1371/journal.pmed.0030328. PMID:16903777.

Cazelles, B., Chavez, M., Berteaux, D., Ménard, F., Vik, J.O., Jenouvrier, S., and Stenseth, N.C. 2008. Wavelet analysis of ecological time series. Oecologia, **156**: 287–304. doi:10.1007/s00442-008-0993-2. PMID:18322705.

Cleland, E.E., Chuine, I., Menzel, A., Mooney, H.A., and Schwartz, M.D. 2007. Shifting plant phenology in response to global change. Trends Ecol. Evol. **22**: 357–365. doi:10.1016/j.tree.2007.04.003. PMID:17478009.

Cook, E.R., and Holmes, R.L. 1984. Program ARSTAN user manual: laboratory of tree ring research. University of Arizona, Tucson, Ariz.

Cook, E.R., and Peters, K. 1981. The smoothing spline: a new approach to standardizing forest interior tree-ring width series for dendroclimatic studies. Tree-Ring Bull. **41**: 45–53.

Cook, E.R., Briffa, K., Shiyatov, S., and Mazepa, V. 1990. Tree ring standardization and growth-trend estimation. *In* Methods of dendrochronology. *Edited by* E.R. Cook and L.A. Kairiukstis. Kluwer Academic Publishers, Dordrecht, Netherlands. pp. 104–123. doi:10.1007/978-94-015-7879-0.

Corona, C., Edouard, J.-L., Guibal, F., Guiot, J., Bernard, S., Thomas, A., and Denelle, N. 2011. Long-term summer (AD751–2008) temperature fluctuation in the French Alps based on tree-ring data. Boreas, **40**(2): 351–366. doi:10.1111/j.1502-3885.2010.00185.x.

Delamaire, S. 2009. Structuration génétique des populations de tordeuse du mélèze, *Zeiraphera diniana* (Lepidoptera: Tortricidae), dans l'espace et dans le temps. Ph.D. thesis, University of Orléans, Orléans, France.

Delamaire, S., Esselink, G.D., Samiei, L., Courtin, C., Magnoux, E., Rousselet, J., and Smulders, M.J.M. 2010. Isolation and characterization of six microsatellite loci in the larch budmoth *Zeiraphera diniana* (Lepidoptera: Tortricidae). Eur. J. Entomol. **107**: 267–269. doi:10.14411/eje.2010.034.

Dormont, L., Baltensweiler, W., Choquet, R., and Roques, A. 2006. Larch- and pine-feeding host races of the larch bud moth (*Zeiraphera diniana*) have cyclic and synchronous population fluctuations. Oikos, **115**(2): 299–307. doi:10.1111/j.2006.0030-1299.15010.x.

Dullinger, S., Gattringer, A., Thuiller, W., Moser, D., Zimmermann, N.E., Guisan, A., Willner, W., Plutzar, C., Leitner, M., Mang, T., Caccianiga, M., Dirnböck, T., Ertl, S., Fischer, A., Lenoir, J., Svenning, J.-C., Psomas, A., Schmatz, D.R., Silc, U., Vittoz, P., and Hülber, K. 2012. Extinction debt of high-mountain plants under twenty-first-century climate change. Nat. Clim. Change, **2**: 619–622. doi:10.1038/nclimate1514.

Edouard, J.L., Guibal, F., Nicault, A., Rathgeber, C., Tessier, L., Thomas, A., and Wicha, S. 2002. Arbres subfossiles (*Pinus cembra*, *Pinus uncinata* et *Larix decidua*) et évolution des forêts d'altitude dans les Alpes Françaises au cours de l'Holocène: approche dendroécologique. Final Proceedings, Equilibre et rupture dans les écosystèmes depuis 20000 ans en Europe de l'Ouest. Presses Universitaires Francomtoises, Besançon, France. pp. 403–411.

Edouard, J.-L., Corona, C., Thomas, A., Guibal, F., and Denelle, N. 2009. Le Petit Age Glaciaire dans les cernes de croissance des arbres des Alpes françaises. Approche dendrochronologique. Archéologie du Midi médiéval, **27**: 169–177.

Edouard, J.-L., Corona, C., Thomas, A., and Touflan, P. 2010. Vieux arbres vivants et arbres morts (mélèzes, *Larix decidua* Mill.; pins cembro, *Pinus cembra* L.) témoins des forêts du passé dans les Alpes du Sud : approche dendrochronologique d'un patrimoine. *In* Proceedings of Biodiversité, Naturalité et Humanité. Pour inspirer la gestion des forêts, Chambéry, France, 27–31 October 2008. *Edited by* D. Vallauri, J. André, J.-C. Génot, J.-P. De Palma, and R. Eynard-Machet. Editions Lavoisier – TEC and DOC. pp. 141–145.

Engler, R., Randin, C.F., Thuiller, W., Dullinger, S., Zimmermann, N.E., Araujo, M.B., Pearman, P.B., Le Lay, G., Piedallu, C., Albert, C.H., Choler, P., Coldea, G., De Lamo, X., Dirnbock, T., Gegout, J.C., Gomez-Garcia, D., Grytnes, J.A., Heegaard, E., Hoistad, F., Nogues-Bravo, D., Normand, S., Puscas, M., Sebastia, M.T., Stanisci, A., Theurillat, J.P., Trivedi, M.R., Vittoz, P., and Guisan, A. 2011. 21st century climate change threatens mountain flora unequally across Europe. Global Change Biol. **17**: 2330–2341. doi:10.1111/j.1365-2486.2010.02393.x.

Esper, J., Büntgen, U., Frank, D.C., Nievergelt, D., and Liebhold, A. 2007. 1200 years of regular outbreaks in alpine insects. Proc. R. Soc. B, **274**: 671–679. doi:10.1098/rspb.2006.0191. PMID:17254991.

Fleming, R.A., and Candau, J.-N. 1998. Influences of climatic change on some ecological processes of an insect outbreak system in Canada's boreal forests and the implications for biodiversity. Environ. Monit. Assess. **49**: 235–249. doi:10.1023/A:1005818108382.

Fritts, H.C. 1976. Tree rings and climate. Academic Press, London.

Grinsted, A., Moore, J.C., and Jevrejeva, S. 2004. Application of the cross wavelet transform and wavelet coherence to geophysical time series. Nonlin. Processes Geophys. **11**: 561–566. doi:10.5194/npg-11-561-2004.

Grossmann, A., and Morlet, J. 1984. Decomposition of Hardy functions into square integrable wavelets of constant shape. SIAM J. Math. Anal. **15**(4): 723–736. doi:10.1137/0515056.

Grossmann, A., Kronland-Martinet, R., and Morlet, J. 1989. Reading and understanding continuous wavelet transforms. *In* Wavelets, time-frequency methods and phase space. *Edited by* J.-M. Combes, A. Grossmann, and P. Tchamitchian. Springer-Verlag, Berlin. pp. 2–20. doi:10.1007/978-3-642-97177-8_1.

Ims, R.A., Henden, J.A., and Killengreen, S.T. 2008. Collapsing population cycles. Trends Ecol. Evol. **23**: 79–86. doi:10.1016/j.tree.2007.10.010. PMID:18191281.

Intergovernmental Panel on Climate Change (IPCC). 2007. Regional climate projections. *In* Contribution of Working Group I to the Fourth Assessment Report of the Intergovernmental Panel on Climate Change, Climate Change The Physical Science Basis. *Edited by* S. Solomon, D. Qin, M. Manning, Z. Chen, M. Marquis, K.B. Avery, M. Tignor, and H.L. Miller. Cambridge University Press, Cambridge, UK.

Jepsen, J.U., Hagen, S.B., Ims, R.A., and Yoccoz, N.G. 2008. Climate change and outbreaks of the geometrids *Operophtera brumata* and *Epirrita autumnata* in subarctic birch forest: evidence of a recent outbreak range expansion. J. Anim. Ecol. **77**(2): 257–264. doi:10.1111/j.1365-2656.2007.01339.x. PMID:18070041.

Johnson, D.M., Bjørnstad, O.N., and Liebhold, A.M. 2004. Landscape geometry and travelling waves in the larch budmoth. Ecol. Lett. **7**: 967–974. doi:10.1111/j.1461-0248.2004.00659.x.

Johnson, D.M., Büntgen, U., Frank, D.C., Kausrud, K., Haynes, K.J., Liebhold, A.M., Esper, J., and Stenseth, N.C. 2010. Climatic warming disrupts recurrent Alpine insect outbreaks. Proc. Natl. Acad. Sci. U.S.A. **107**(47): 20576–20581. doi:10.1073/pnas.1010270107. PMID:21059922.

Jolliffe, I.T. 2002. Principal component analysis. Wiley StatsRef: Statistics Reference Online. doi:10.1002/9781118445112.stat06472.

Kneeshaw, D., Sturtevant, B.R., Cooke, B., Work, T., Pureswaran, D., DeGrandpre, L., and MacLean, D. 2015. Insect disturbances in forest ecosystems. *In* Routledge handbook of forest ecology. *Edited by* K.S.-H. Peh, R.T. Corlett, and Y. Bergeron. Taylor and Francis Group, New York.

Labat, D. 2010. Cross wavelet analyses of annual continental freshwater discharge and selected climate indices. J. Hydrol. **385**: 269–278. doi:10.1016/j.jhydrol.2010.02.029.

Lau, K.-M., and Weng, H. 1995. Climate signal detection using wavelet transform: how to make a time series sing. Bull. Am. Meteorol. Soc. **76**: 2391–2402. doi:10.1175/1520-0477(1995)076<2391:CSDUWT>2.0.CO;2.

Lenoir, J., Gégout, J.C., Marquet, P.A., de Ruffray, P., and Brisse, H. 2008. A significant upward shift in plant species optimum elevation during the 20th century. Science, **320**: 1768–1771. doi:10.1126/science.1156831. PMID:18583610.

Lindner, M., Maroschek, M., Netherer, S., Kremer, A., Barbati, A., Garcia-Gonzalo, J., Seidl, R., Delzon, S., Corona, P., Kolström, M., Lexer, M.J., and Marchetti, M. 2010. Climate change impacts, adaptive capacity, and vulnerability of European forest ecosystems. For. Ecol. Manage. **259**(4): 698–709. doi:10.1016/j.foreco.2009.09.023.

Logan, J.A., Régnière, J., Gray, D.R., and Munson, A.S. 2007. Risk assessment in the face of a changing environment: gypsy moth and climate change in Utah. Ecol. Appl. **17**: 101–117. doi:10.1890/1051-0761(2007)017[0101:RAITFO]2.0.CO;2. PMID:17479838.

Maggini, R., Lehmann, A., Kéry, M., Schmid, H., Beniston, M., Jenni, L., and Zbinden, N. 2011. Are Swiss birds tracking climate change? Detecting elevational shifts using response curve shapes. Ecol. Modell. **222**: 21–32. doi:10.1016/j.ecolmodel.2010.09.010.

Maraun, D., and Kurths, J. 2004. Cross wavelet analysis: significance testing and pitfalls. Nonlin. Processes Geophys. **11**: 505–514. doi:10.5194/npg-11-505-2004.

Motta, R. 2004. Stand history reconstruction, spatial and temporal growth relationships in two forest stand in the Upper Susa Valley (Piedmont, Italy). Ph.D. thesis, University of Aix – Marseille III, Provence, France.

Nash, T.H., Fritts, H.C., and Stokes, M.A. 1975. A technique for examining nonclimatic variation in widths of annual tree rings with special reference to air pollution. Tree-Ring Bull. **35**: 15–24. doi:10150/260112.

Netherer, S., and Schopf, A. 2010. Potential effects of climate change on insect herbivores in European forests — general aspects and the pine processionary moth as specific example. For. Ecol. Manage. **259**(4): 831–838. doi:10.1016/j.foreco.2009.07.034.

Nola, P., Morales, M., Motta, R., and Villalba, R. 2006. The role of larch budmoth (*Zeiraphera diniana* Gn.) on forest succession in a larch (*Larix decidua* Mill.) and Swiss stone pine (*Pinus cembra* L.) stand in the Susa Valley (Piedmont, Italy). Trees, **20**: 371–382. doi:10.1007/s00468-006-0050-x.

Parmesan, C. 1996. Climate and species' range. Nature, **382**: 765–766. doi:10.1038/382765a0.

Parmesan, C. 2006. Ecological and evolutionary responses to recent climate change. Annu. Rev. Ecol. Evol. Syst. **37**: 637–669. doi:10.1146/annurev.ecolsys.37.091305.110100.

Peterson, D.W., Peterson, D.L., and Ettl, G.J. 2002. Growth responses of subalpine fir to climatic variability in the Pacific Northwest. Can. J. For. Res. **32**: 1503–1517. doi:10.1139/x02-072.

Petitcolas, V., and Rolland, C. 1998. Comparaison dendroécologique de *Larix decidua* Mill., *Pinus cembra* L. et *Pinus uncinata* Mill. ex Mirb., dans l'étage subalpin du briançonnais (Hautes-Alpes, France). Ecologie, **29**(1–2): 305–310.

Ranta, E., Lundberg, P., Kaitala, V., and Stenseth, N.C. 2002. On the crest of a population wave. Science, **298**: 973–974. doi:10.1126/science.1078707. PMID:12411689.

Richman, M.B. 1986. Rotation of principal components. Int. J. Climatol. **6**(3): 293–335. doi:10.1002/joc.3370060305.

Robinet, C., and Roques, A. 2010. Direct impacts of recent climate warming on insect populations. Integrative Zoology, **5**: 132–142. doi:10.1111/j.1749-4877.2010.00196.x. PMID:21392331.

Rolland, C., Baltensweiler, W., and Petitcolas, V. 2001. The potential for using *Larix decidua* ring widths in reconstructions of larch budmoth (*Zeiraphera diniana*) outbreak history: dendrochronological estimates compared with insect surveys. Trees, **15**(7): 414–424. doi:10.1007/s004680100116.

Roques, A. (*Editor*). 2015. Processionary moths and climate change: an update. Springer, Dordrecht, Netherlands. doi:10.1007/978-94-017-9340-7.

Roques, A., and Goussard, F. 1982. Améliorations de la technique de prévision de pullulation de la tordeuse du mélèze *Zeiraphera diniana* Guénée (Lép. Tortricidae). Acta Oecol., Oecol. Appl. **3**: 35–45.

Saracco, G. 1994. Propagation of transient waves through a stratified fluid medium: wavelet analysis of a nonasymptotic decomposition of the propagator. Part I. Spherical waves through a two-layered system. J. Acoust. Soc. Am. **95**(3): 1191–1205. doi:10.1121/1.408563.

Saracco, G., Sessarego, J.-P., Sageloli, J., Guillemain, P., and Kronland-Martinet, R. 1991. Extraction of modulation laws of elastic shells by the use of the wavelet transform. *In* Research notes in applied mathematics: wavelets and applications. *Edited by* Y. Meyer. Masson-Springer. pp. 61–68.

Saracco, G., Thouveny, N., Bourlès, D.L., and Carcaillet, J.T. 2009. Extraction of non-continuous orbital frequencies from noisy insolation data and from palaeoproxy records of geomagnetic intensity using the phase of continuous wavelet transforms. Geophys. J. Int. **176**(3): 767–781. doi:10.1111/j.1365-246X.2008.04057.x.

Saulnier, M. 2012. Histoire et dynamique de la de la forêt subalpine dans les Alpes du Sud (Briançonnais, Queyras): approches pédoanthracologique et dendrochronologique. Ph.D. thesis, University of Aix – Marseille III, Provence, France.

Saulnier, M., Edouard, J.-L., Corona, C., and Guibal, F. 2011. Climate/growth relationships in a *Pinus cembra* high-elevation network in the southern French Alps. Ann. For. Sci. **68**(1): 189–200. doi:10.1007/s13595-011-0020-3.

Serre, F. 1978. The dendroecological value of the European larch (*Larix decidua* Mill.) in the French maritime Alps. Tree-Ring Bull. **38**: 25–34.

Setz, T. 2011. Wavelet analysis on stochastic time series: a visual introduction with an examination of long term financial time series. Semester thesis, ETH Zürich, Zürich, Switzerland.

Speer, J.H. 2010. Fundamentals of tree-ring research. University of Arizona Press, Tucson, Ariz.

Stokes, M.A., and Smiley, T.L. 1968. An introduction to tree-ring dating. University of Arizona Press, Tucson, Ariz.

Sturm, M., Racine, C., and Tape, K. 2001. Climate change: increasing shrub abundance in the Arctic. Nature, **411**: 546–547. doi:10.1038/35079180. PMID:11385559.

Swetnam, T.W., Thompson, M.A., and Kennedy Sutherland, E. 1985. Using dendrochronology to measure radial growth of defoliated trees. USDA Forest Service, Agriculture Handbook No. 639.

Tessier, L. 1986. Chronologie de mélèzes des Alpes et Petit Age Glaciaire. Dendrochronologia, **4**: 97–113.

Torrence, C., and Compo, G.P. 1998. A practical guide to wavelet analysis. Bull. Am. Meteorol. Soc. **79**: 61–78. doi:10.1175/1520-0477(1998)079<0061:APGTWA>2.0.CO;2.

Valero, H.P., and Saracco, G. 2005. 3-D seismic endoscopy: multiscale analysis and dynamic azimuthal filtering of borehole waves. Geophys. J. Int. **161**: 813–828. doi:10.1111/j.1365-246X.2005.02616.x.

Volney, W.J.A., and Fleming, R.A. 2000. Climate change and impacts of boreal forest insects. Agric., Ecosyst. Environ. **82**: 283–294. doi:10.1016/S0167-8809(00)00232-2.

Weber, U.M. 1997. Dendroecological reconstruction and interpretation of larch budmoth (*Zeiraphera diniana*) outbreaks in two central alpine valleys of Switzerland from 1470–1990. Trees, **11**(5): 277–290. doi:10.1007/PL00009674.

Wigley, T.M.L., Briffa, K.R., and Jones, P.D. 1984. On the average value of correlated time series, with applications in dendroclimatology and hydrometeorology. J. Clim. Appl. Meteorol. **23**: 201–213. doi:10.1175/1520-0450(1984)023<0201:OTAVOC>2.0.CO;2.

Williams, D.W., and Liebhold, A.M. 1995. Herbivorous insects and global change: potential changes in the spatial distribution of forest defoliator outbreaks. J. Biogeogr. **22**: 665–671. doi:10.2307/2845968.